

Generalised Image Outpainting with U-Transformer

Penglei Gao ^{*1}, Xi Yang ^{*2}, Rui zhang¹, Kaizhu Huang ^{†2}, and Yujie Geng²

¹Department of Science

²Department of Intelligent Science

Xi'an Jiaotong-Liverpool University. Suzhou, 215123, China.

Penglei.gao19,Yujie.geng20@student.xjtlu.edu.cn,
xi.yang01,rui.zhang02,kaizhu.huang @xjtlu.edu.cn

March 8, 2022

Abstract

While most present image outpainting conducts horizontal extrapolation, we study the generalised image outpainting problem that extrapolates visual context all-side around a given image. To this end, we develop a novel transformer-based generative adversarial network called U-Transformer able to extend image borders with plausible structure and details even for complicated scenery images. Specifically, we design a generator as an encoder-to-decoder structure embedded with the popular Swin Transformer blocks. As such, our novel framework can better cope with image long-range dependencies which are crucially important for generalised image outpainting. We propose additionally a U-shaped structure and multi-view Temporal Spatial Predictor network to reinforce image self-reconstruction as well as unknown-part prediction smoothly and realistically. We experimentally demonstrate that our proposed method could produce visually appealing results for generalized image outpainting against the state-of-the-art image outpainting approaches.

1 Introduction

Reviewed from the previous works, most image outpainting conducts horizontal extrapolation, which expands the unknown-part image on one side. Differently, we study the generalised image outpainting problem that extrapolates visual context all-side around a given image, as shown in Fig. 1. Extrapolation on all sides has to handle the spatial relationship in both the horizontal and vertical directions (in Fig. 1(b)) considering the size expansion and one-side constraints. Unlike image inpainting [19, 32, 30], which makes use of rich contextual information, outpainting requires extrapolation to unknown image regions with less contextual information [12]. Dealing with such outpainting tasks, one has to predict and refill the missing regions with features totally absent from the input image [13]. This leads to challenges to generate the exact and smooth scenes around the image for all boundaries as follows: 1) the missing features should be located relative to the spatial location of both near and distant features in the output; 2) the conditional input could be spatially distant from the missing regions to be predicted, which is difficult due to the lack of neighbouring ground truths. Thus, the interesting and meaningful topic is to design an appropriate framework to reconstruct and generate high-quality images that maintain the potential con-

^{*}Equal contribution

[†]Corresponding author

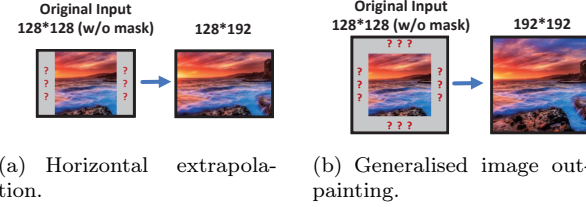


Figure 1: Illustration of image outpainting.

sistency in spatial configuration and semantic content with the original images [31, 16].

The existing horizontal and generalised image outpainting methods still suffer from blunt structures and abrupt colours when extrapolating the unknown regions of the images, although they have achieved solid performance [31, 12, 29, 26]. The potential reason could be the fact that the Encoder-Decoder architecture (Fig. 2(a)) tends to ignore the spatial and semantic consistency only considering the semantic relationship between original and generated images. The authors in [31, 16] exploited a U-Net structure (Fig. 2(b)) allowing for the decoder to generate a more correlated prediction from the encoder involving the spatial relation. As a matter of fact, all the existing deep learning-based image outpainting methods are based on convolutional neural network (CNN). Such CNN backbone however suffers from intrinsic locality and lacks the ability of capturing global features and representing long-range relations. The U-Net structure is limited in extracting the long-range semantic information interaction as well [2].

To better cope with image long-range dependencies and spatial relationships among predicted regions and conditional input, we develop a novel transformer-based generative adversarial network (GAN) called U-Transformer in this paper. Unlike present CNN-based outpainting models, U-Transformer is the first model built on the transformer architecture able to extend image borders seamlessly. Concretely, we design our U-Transformer with the Swin Transformer [3] blocks, which transform an image into a vector by using a flattened patch method and then replace the CNNs with window self-attention (WSA). WSA controls the com-

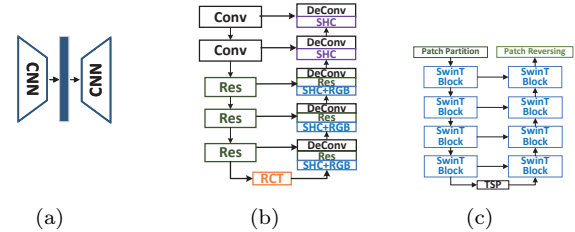


Figure 2: Image outpainting architectures. (a) Commonly used CNN-based Encoder-Decoder architecture; (b) U-Net architecture for Horizontal extrapolation task; (c) Proposed U-Transformer for Generalised images outpainting task.

putation area by a window size, which makes the network easier to obtain global features for image long-range dependencies, especially for the predicted corner regions. We propose additionally a U-shaped structure and multi-view Temporal Spatial Predictor (TSP) to reinforce image self-reconstruction as well as unknown-part prediction (Fig. 2), both of which prove vital for generating image outpainting smoothly and realistically.

On the practical front, the transformer-based encoder and decoder with Swin Transformer blocks are used to extract context features. The shifted window scheme has greater efficiency for non-overlapping patches computation in self-attention while allowing for cross-window connection. Moreover, the U-shaped structure has the ability to enhance the spatial and semantic consistency for higher-quality image generation at the same layer level between encoder and decoder. As for the bottleneck, the designed TSP module connects the encoder and decoder to capture the temporal information and spatial consistency among decomposed feature maps. Modelling the temporal relations and spatial correlations by multi-view recurrent neural network (RNN) and self-attention block could help generate the outside regions smoothly and realistically. Specifically, the output feature map of the encoder is divided into several small feature bars, which share a Long Short Term Memory (LSTM) [8] block. Then, each predicted feature bar is used to learn the spatial correlations via

self-attention. Due to the fidelity expected at the higher resolution, Relativistic Average Least-Square GAN (RaLSGAN) [11] is involved in making the generated images indistinguishable from the real images.

Our contributions are summarized in three-folds:

- To the best of our knowledge, the proposed U-Transformer is the first transformer-based image outpainting framework. The Swin transformer blocks are able to obtain global features and keep high resolutions. A U-shaped structure and TSP module can reinforce image self-reconstruction as well as unknown-part prediction smoothly and realistically.
- The TSP module connects encoder and decoder, which transfers incomplete latent features considering the temporal relations and spatial correlations by the multi-view LSTM and self-attention blocks.
- U-Transformer produces visually appealing results for generalised image outpainting against the state-of-the-art image outpainting approaches. It also outperforms the competitors in terms of quantitative results.

2 Related Work

2.1 Image Outpainting

Image outpainting fills the external regions of an image naturally and generates a high-quality larger natural image. Since the generated image usually resides beyond the boundaries of an original image and has insufficient contextual information, this task has two main challenges. One is to maintain the content and spatial of the generated region consistent with the original input. Another one is to generate high-quality larger images. Typically, image outpainting methods have been addressed only in a few studies on two derived tasks, horizontal outpainting and generalised outpainting [26]. Inspired from image inpainting methods, the image outpainting task was refocused by Mark Sabini and Gili Rusak [23] on a deep neural network framework. This effort focused

on enhancing and smoothing the quality of generated images by using GANs and the post-processing methods to perform horizontal outpainting. Hoorick [26] demonstrated that GAN has reasonable extrapolations to generate the similar content of the unknown region with the original image. Wang et al. [29] proposed a Semantic Regeneration Network which learned semantic features directly from a small input image to avoid the bias in the general padding and up-sampling. However, these architectures tend to ignore the spatial and semantic consistency, so that they still suffer from blunt structures and abrupt colours issues. To solve this issue, Yang et al. [31] proposed a Recurrent Content Transfer (RCT) model for temporal content prediction by adopting a single LSTM model as the bottleneck. LSTM was designed to better control the horizontal information prediction for a very long-range image outpainting. To increase the contextual information, Lu et al. [16] and Kim et. al. [12] rearranged the boundary region by switching the outer area of the image into its inner area. Moreover, Ma et al. [17] proposed a two-stage image outpainting framework that decomposed the task into two generation stages, semantic segmentation domain and image domain, to improve the quality and diversity of the output image. However, these latest models are based on convolutional neural networks. Since global information is not well captured, they all have limitations in explicitly modelling long-range dependency.

2.2 Transformer

Transformer was first proposed to solve Natural Language Processing (NLP) tasks by discarding the traditional CNN and RNN structures. The entire network structure was composed of Self-Attention and Feed Forward Neural Network entirely. Inspired by the success in the NLP field, efforts in the last two years made some adaptations of the Transformer architecture to make it suitable for basic visual feature extraction [27]. Self-attentive layers were used to replace some or all of the convolutional layers in ResNet, which achieved better accuracy and sped up the optimization [10, 21]. However, the actual latency was significantly larger than that of convolutional layers.

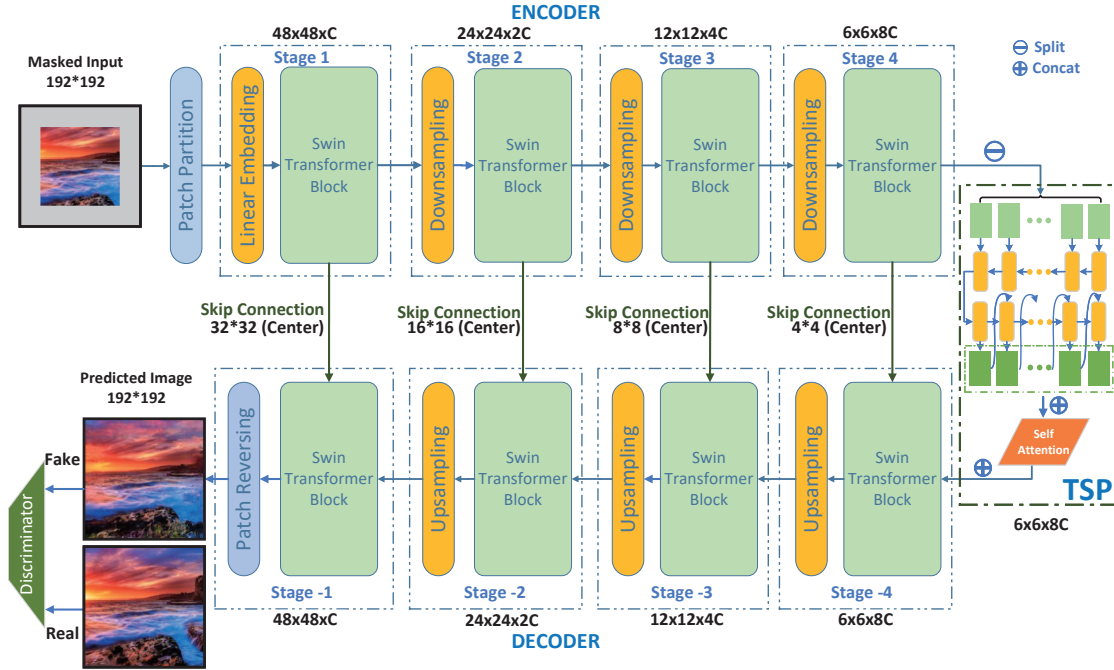


Figure 3: Overview of the U-Transformer for image outpainting consists of swin-transformer encoder-decoder, U-Net alike skip connection and temporal spatial predictor.

tional networks because self-attention was computed within a local window of each pixel. To better achieve the speed-accuracy trade-off on image classification, Vision Transformer (ViT) [3] explored a Transformer with global self-attention to full-size images directly. Meanwhile, other variants of ViT also take efforts to improve the model performance on many vision tasks [33, 6, 4]. Moreover, Liu et al [14] proposed Swin Transformer to extend vision tasks to object detection and semantic segmentation. Swin Transformer involved Shifted window attention to bridge the windows of the preceding layer, which significantly enhanced modelling power as well as achieved lower latency. In particular, Swin Transformer has been extremely successful in the field of medical image segmentation. Cao et al. [1] replaced all the convolution layers with transformer blocks on U-Net structure for image segmentation, achieving better accuracy than [2] which substituted several parts of convolution blocks. To the best of our knowledge,

the proposed U-Transformer is the first Transformer-based image outpainting framework.

3 Methodology

The overall architecture is presented in Fig. 3. The underlying framework relies on a transformer-based encoder-decoder architecture, in which U-Net is utilized to enhance the self-reconstruction of the input images. In the feature prediction stage, we design a multi-view temporal and spatial information fusion approach. The details of each component are described in the following sections.

3.1 Problem Statement

Given an image $I_x \in \mathbb{R}^{h \times w \times 3}$, we aim to extrapolate the outside contents beyond the image boundary with extra m -pixels. The generator will pro-

duce a visually convincing image $I_{pred} \in \mathbb{R}^{h' \times w' \times 3}$, where $h' = h + 2m, w' = w + 2m$. In practice, the outpainted image I_{pred} is generated by mapping a partially masked RGB input image of size $h' \times w'$ with centre image I_x , which is denoted as $I_{mask} \in \mathbb{R}^{h' \times w' \times 3}$. I_{pred} has the same size as I_{mask} , in which the model’s predictions replace the masked part.

3.2 Overall Framework

Our proposed model is a U-Net alike encoder-decoder architecture for generalised image outpainting. Generally, the basic encoder and decoder structures are derived from Swin Transformer [15] by adding extra padding operation in the shifted window self-attention block for both encoder and decoder.

In the encoder \mathcal{E}_{nc} , the masked input images I_m are first split into non-overlapping patches by a patch partition layer with a patch size of 4×4 . The feature dimension of each patch is $4 \times 4 \times 3 = 48$ since each patch’s feature could be considered a combination of the raw pixel RGB values. These patches features will be projected to latent features of dimension C by a linear embedding layer. After the patch embedding, there are $(\frac{H}{4} \times \frac{W}{4})$ patch tokens passed through several Swin Transformer blocks to obtain the hierarchical feature representations. Moreover, a patch merging operation between two adjacent Swin Transformer blocks reduces the token resolution by $2 \times$ down-sampling layer. We additionally apply a linear layer on the newly produced $4C^l$ -dimensional features to convert the dimension to $2C^l$ in the l -th layer.

The decoder \mathcal{D}_{ec} is composed of Swin Transformer blocks with an up-sampling layer and patch reversing block. In contrast to a down-sampling layer, an up-sampling layer operates $2 \times$ up-sampling resolution to expand the feature map. A linear layer is applied to convert the feature dimension of $2C^l$ to $4C^l$ before up-sampling at each layer level. Inspired from U-Net [22], we adopt Skip Connections (SC) to fuse and share the feature information from the encoder to the decoder at the same layer level (details in Section 3.5). The SC could encourage the decoder to learn more accurate representation of cen-

tre reconstruction and generalized prediction taking full advantage of the information extracted from the encoder at each layer.

As for the bottleneck, we design a Temporal Spatial Predictor (TSP) module to propagate the information from input image feature maps to predicted feature maps which connect the encoder and decoder for more accurate outpainted features prediction. The detailed structure will be described in Section 3.4. In addition, the adversarial training is applied to encourage the generator \mathcal{G} consisting of \mathcal{E}_{nc} , TSP and \mathcal{D}_{ec} to output more real images with a discriminator \mathcal{D}_{is} .

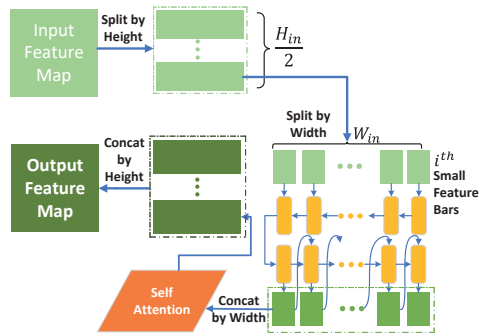


Figure 4: Temporal Spatial Predictor (TSP) structure.

3.3 Swin Transformer

The global computation in standard self-attention makes it feasible to extract global features; however, it also leads to a huge complexity due to the increase in the number of tokens. This makes it impracticable for image processing when representing high-resolution images. For efficient modelling, we leverage Swin Transformer [15] which replaces the standard multi-head self-attention (MSA) module by utilizing shifted windows. The two successive Swin Transformer blocks are connected alternately, containing a window-based multi-head self-attention (W-MSA) module and a shifted-window-based multi-head self-attention (SW-MSA) module, respectively. The windows are arranged to evenly partition the image in a non-overlapping manner in the W-MSA

module. Then, the next SW-MSA module adopts a windowing configuration that is shifted from that of the preceding module. The shifted window partitioning approach captures the cross-relationship between neighbouring non-overlapping windows in the previous layer. Each block consists of a LayerNorm (LN) layer, a 2-layer MLP and GELU activation function with a residual connection between each module. According to the combined window partitioning approach, the consecutive Swin Transformer blocks are formulated as:

$$\begin{aligned}\hat{\mathbf{z}}^l &= \text{W-MSA}(\text{LN}(\mathbf{z}^{l-1})) + \mathbf{z}^{l-1}, \\ \mathbf{z}^l &= \text{MLP}(\text{LN}(\hat{\mathbf{z}}^l)) + \hat{\mathbf{z}}^l, \\ \hat{\mathbf{z}}^{l+1} &= \text{SW-MSA}(\text{LN}(\mathbf{z}^l)) + \mathbf{z}^l, \\ \mathbf{z}^{l+1} &= \text{MLP}(\text{LN}(\hat{\mathbf{z}}^{l+1})) + \hat{\mathbf{z}}^{l+1},\end{aligned}\quad (1)$$

where $\hat{\mathbf{z}}^l$ and \mathbf{z}^l are the output features of the (S)W-MSA module and the MLP module of block l respectively. Following the previous work [9, 10, 20], the similarity of self-attention is computed as:

$$\text{Att}(Q, K, V) = \text{SoftMax}(QK^T / \sqrt{d} + B)V, \quad (2)$$

where $Q, K, V \in \mathbb{R}^{M^2 \times d}$ represent the *query*, *key* and *value* matrices and $B \in \mathbb{R}^{M^2 \times M^2}$ is relative position bias. M^2 is the number of patches in a window and d is the dimension of *query/key*. The bias B are taken from a smaller sized bias matrix $\hat{B} \in \mathbb{R}^{(2M-1)(2M-1)}$.

3.4 Temporal Spatial Predictor

The TSP module is designed for efficient information propagation and representation, considering the potentially temporal and spatial evolution in images. As shown in Fig. 4, we vertically decompose the feature map from the encoder component into several small feature bars. Each small feature bar is split into a sequence in the width dimension and then processed by a 2-layer LSTM block to transfer this sequence to a new feature bar in the prediction region to capture the temporal information. After that, the new feature bar and its neighbouring feature bars as *value* and *query/key* will be processed by a standard multi-head self-attention to regulate the predicted features

with the spatial information. In the end, the predicted feature bars are concatenated in the height dimension, forming the predicted feature map with a normalization layer. In TSP, the size of the prediction region is adapted by the width of feature map in 1-step prediction. The height of the feature map adapts to the number of small feature bars. According to the size of the masked feature map, the TSP module could output target feature size by iterating the LSTM block and self-attention block to generate images with high quality.

3.5 Skip Connection

To enhance the modelling ability of the decoder, we leverage skip connections between encoder and decoder. The un-masked centre feature maps at each encoder layer level are merged to the decoder layer level to share information. Given a feature from the l -th layer in encoder fe_{h^l, w^l, c^l} and a feature from the corresponding layer in decoder fd_{h^l, w^l, c^l} , SC computes a new feature fd'_{h^l, w^l, c^l} as follows:

$$fd'_{h^l_{cen}, w^l_{cen}, c^l} = (fe_{h^l_{cen}, w^l_{cen}, c^l} + fd_{h^l_{cen}, w^l_{cen}, c^l}) / 2. \quad (3)$$

Then $fd'_{h^l, w^l, c^l} :=$ substitute the center part of fd_{h^l, w^l, c^l} with $fd'_{h^l_{cen}, w^l_{cen}, c^l}$, where h^l_{cen}, w^l_{cen} represent the center size of a given feature map.

3.6 Loss Function

Our loss function consists of four parts: pixel reconstruction loss, feature reconstruction loss, texture consistency loss and adversarial loss. The pixel reconstruction loss captures the logical coherence between the generated images and ground truth from the overall structure, which focuses on low-order information. The feature reconstruction loss is responsible for enhancement of self-reconstruction in latent space. The texture consistency loss is utilized to encourage similar feature distribution between fake images and real images. The adversarial loss learns to make the predicted images more real due to high-order information capturing.

Pixel Reconstruction Loss We use an L1 distance between ground truth image I_{gt} and generated

image I_{pred} as the pixel reconstruction loss denoted as $\mathcal{L}_{rec}(X)$,

$$\mathcal{L}_{rec}(I_{mask}) = \|I_{gt} - I_{pred}\|_1. \quad (4)$$

Feature Reconstruction Loss When performing self-reconstruction, we could extract the feature map of the un-masked centre ground truth image I_x via the encoder \mathcal{E}_{nc} , and encourage the predicted centre feature from the TSP module to be identical to it. The feature reconstruction loss \mathcal{L}_{feat_rec} is defined as:

$$\mathcal{L}_{feat_rec} = \|f_{cen} - \mathcal{E}_{nc}(I_x)\|_1, \quad (5)$$

where f_{cen} is the centre part of the output from the TSP module.

Texture Consistency Loss According to previous works of impainting, outpainting, and image translation [18, 28, 29], we add the regularization of implicit diversified Markov random fields (IDMRF) to our loss function. IDMRF loss models the feature difference between $F(I_{fake})$ and $F(I_{real})$ and pushes I_{fake} to have similar feature distribution as ground truth in self-reconstruction, where F is a pretrained feature extractor. This IDMRF loss is represented as:

$$\mathcal{L}_{mrf} = \text{IDMRF}(I_{fake}, I_{real}), \quad (6)$$

where the computation of IDMRF is identical to the one in [28]. We use the layers $relu3_2$ and $relu4_2$ of a pretrained VGG19 [25] network as the feature extractor F .

Adversarial Loss The adversarial losses for balancing the discriminator \mathcal{D}_{is} and the generator \mathcal{G} are defined as follows:

$$\begin{aligned} \mathcal{L}_{GAN}^{I_{gt}} = & \mathbb{E}_{I_{mask} \sim p(I_{mask})} [\log(1 - \mathcal{D}_{is}(\mathcal{G}(I_{mask})))] \\ & + \mathbb{E}_{I_{gt} \sim p(I_{gt})} [\log \mathcal{D}_{is}(I_{gt})]. \end{aligned} \quad (7)$$

In the experimental implementation, we leverage the RaLSGAN [11] to perform adversarial learning for the discriminator because of its advantages of having more stable training and generating higher-quality images. The details about RaLSGAN can be found in the supplementary material.

Overall Objectives We jointly train the generator and discriminator to optimize the overall objective, which is a weighted sum of the aforementioned

objectives:

$$\begin{aligned} \mathcal{L} = & \min_{\mathcal{G}} \max_{\mathcal{D}_{is}} \mathcal{L}(\mathcal{G}, \mathcal{D}_{is}) \\ = & \lambda_{rec} \mathcal{L}_{rec} + \lambda_{feat_rec} \mathcal{L}_{feat_rec} \\ & + \lambda_{mrf} \mathcal{L}_{mrf} + \mathcal{L}_{GAN}^{I_{gt}}. \end{aligned} \quad (8)$$

In our experiments, we set $\lambda_{rec} = 20$, $\lambda_{feat_rec} = 1$, $\lambda_{mrf} = 0.5$, and $\lambda_{adv} = 1$.

4 Experiments

4.1 Dataset

In our experiments, we use the scenery dataset proposed by [31] to conduct the generalised outpainting for comparison. The scenery dataset consists of about 5,000 images for training and 1,000 images for testing. In addition, we prepare a new building facades dataset in different styles consisting of diverse and complicated building architecture. There are about 16,000 images in the training set and 1,500 images in the testing set. All the images are collected on the internet. More details about the building dataset could be found in the supplementary material.

4.2 Implementation Details

In our experimental setting, we first pre-process the data by resizing the original images to 192×192 as ground truth images I_{gt} . The masked input images I_{mask} are obtained by centre cropping operation on I_{gt} with size 128×128 and expanding masks around the images with extra 32-pixels. The total output size is 2.25 times that of the input, indicating that over half of all pixels will be generated. For both encoder and decoder, the number of layers is 4, the corresponding depth is $[2, 2, 6, 2]$ and the number of head is $[3, 6, 12, 24]$ for each layer. The window size is set to $M = 7$ and the query dimension of each head is $d = 32$. The embedding dimension C is 96. The experiments are implemented with PyTorch 1.7 and trained on a single NVidia RTX3090. We use Frechet Inception distance (FID) [7], Inception Score (IS) [24], peak signal-to-noise ratio (PSNR),

Dataset	Scenery					Building				
Metrics	FID↓	IS↑	PSNR↑	SSIM↑	Time	FID↓	IS↑	PSNR↑	SSIM↑	Time
NSIPO[31]	25.977	3.059	21.089	0.744	44.190	30.465	4.153	18.314	0.694	44.590
SRN[29]	47.781	2.981	22.440	0.751	11.960	38.644	3.862	18.588	0.671	12.240
IOH[26]	32.107	2.886	22.286	0.665	4.160	49.481	3.924	18.431	0.623	4.270
U-Transformer	20.575	3.249	23.007	0.777	46.810	30.542	4.189	18.828	0.703	47.060

Table 1: Quantitative results and inference time (ms/image) compared with other outpainting methods.

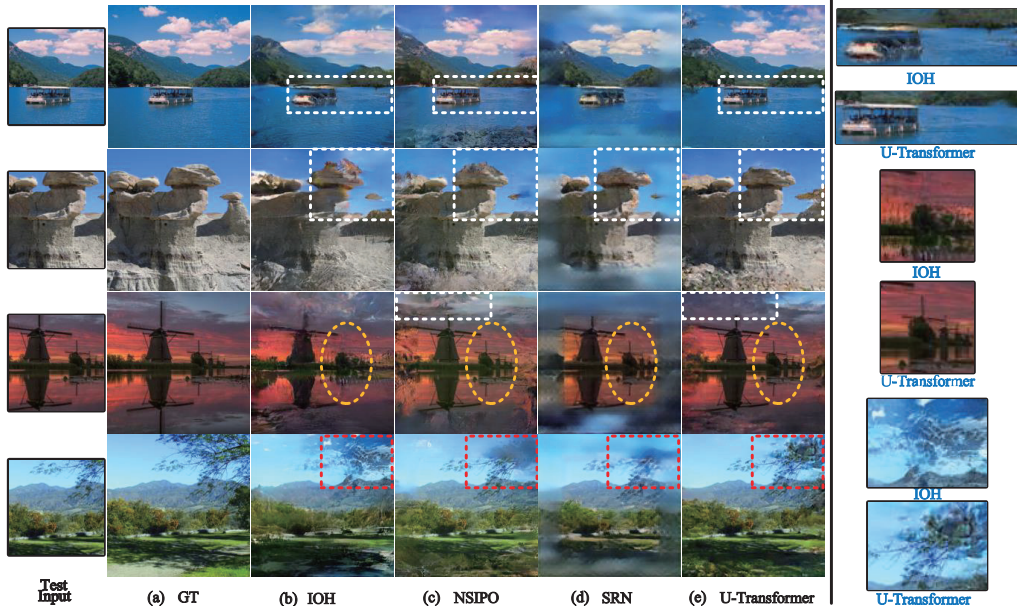


Figure 5: Qualitative results compared with other outpainting methods on scenery dataset.

and structural similarity index measure (SSIM) metrics for quantitative comparison. The implemented codes are provided in the supplementary material.

4.3 Experimental Results

In the following, we first compare the proposed model with the previous state-of-the-art on generalized image outpainting. Then, we ablate the important designs of U-Transformer. We choose three baseline models for comparison with quantitative and qualitative evaluation. Model IOH [26] and SRN [29] are current generalised image outpainting methods. IOH is an encoder-decoder structure by using CNN

with adversarial loss. SRN leverages two encoder-decoder structures for feature expansion and context prediction. NSIPO [31] uses ResNet [5] as backbone and equipping with skip horizontal connection (SHC) and recurrent content transfer (RCT) for horizontal extrapolation.

4.3.1 Quantitative Results

The quantitative results of evaluation metrics FID, IS, PSNR, SSIM and inference time against other state-of-the-art models on the scenery and building datasets are described in Table 1. Notably, our proposed U-Transformer achieves the best scores

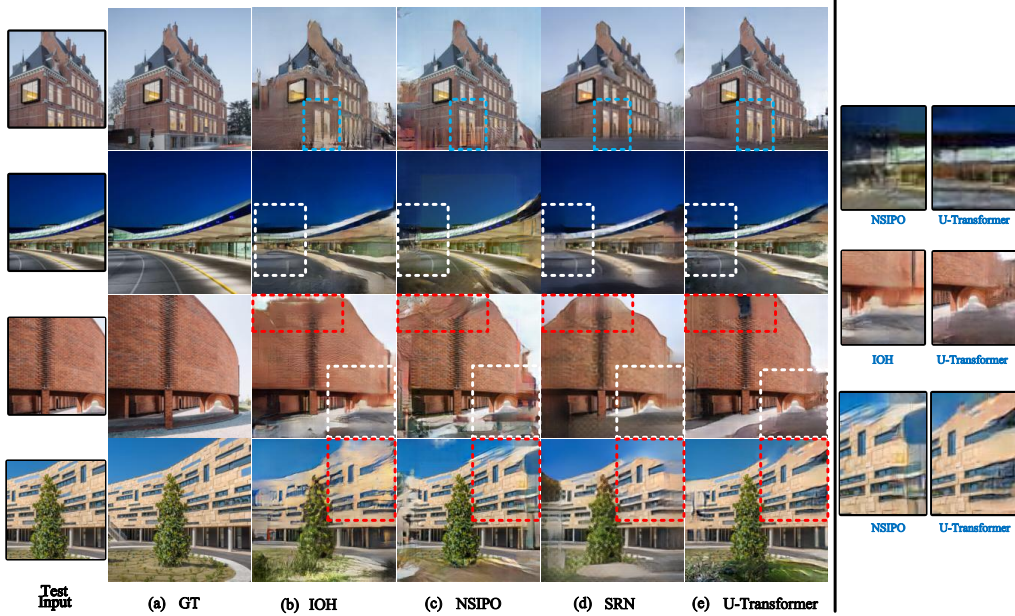


Figure 6: Qualitative results compared with other outpainting methods on building dataset.

among all the evaluation metrics, showing that our transformer-based network could model the global and distant relations for all-side extrapolations.

4.3.2 Qualitative Results

Fig. 5 and Fig. 6 show some examples of generalised outpainting results on the scenery and building datasets indicating that our proposed model generates visually appealing results, especially for the four corner regions. The horizontal outpainting method NSIPO extrapolates one side of a given image, limiting generalised outpainting. The BCT block in NSIPO is explicitly designed to predict feature maps horizontally, which expands features for all four sides respectively in generalised outpainting. The edges between the expanded part and the original image are apparent and the predicted regions tend to be distorted frequently. Nevertheless, our model weakens the sense of edges between the original and generated pixels and makes the expanded part more realistic. Our model also achieves better results than SRN and

IOH which are both CNN-based generalised image outpainting methods. They still suffer from blurri ness and unsatisfying extrapolation in the generated images. Compared to IOH, our model could generate better-reconstructed windmills and rocks marked in orange circle in column (b) and (e) of Fig. 5. Compared to NSIPO, the predicted regions of our model are more smooth and real with reasonable content in column (c) and (e) of Fig. 6. Moreover, the dotted box indicates that our model generates more realistic and seamless images in terms of details, e.g. the trees, rocks and rivers predicted in column (e) of Fig. 5. Due to the page limitation, more visual results are presented in the supplementary material.

4.4 Ablation Study

We performed an ablation study to demonstrate the necessity of each component in the proposed U-Transformer. Table 2 shows the quantitative results with different model variants where they are trained with the same training strategy on the scenery

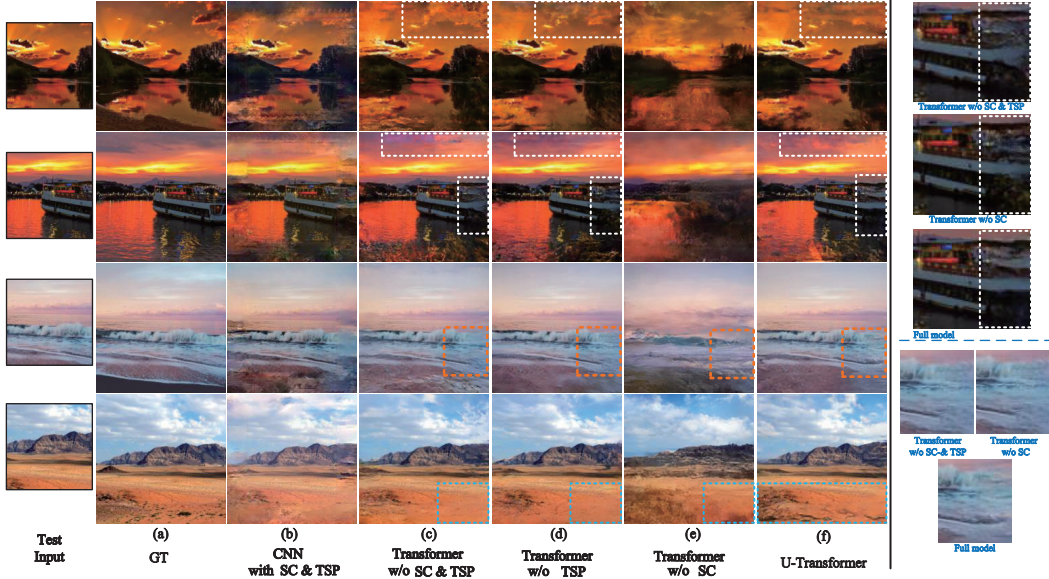


Figure 7: Visual results of ablation study on Scenery dataset.

	FID \downarrow	IS \uparrow	PSNR \uparrow	SSIM \uparrow
w/o Trans	37.934	2.991	22.658	0.743
w/o SC&TSP	29.390	3.092	23.333	0.768
w/o SC	92.038	2.345	20.895	0.554
w/o TSP	25.005	3.215	23.451	0.782
Full model	20.575	3.249	23.007	0.777

Table 2: Ablation study of each component in our proposed model. w/o Trans: Replacing the transformer structure with CNN backbone. w/o SC&TSP: Removing both the SC and TSP modules. w/o SC: Removing the U-Net skip connection. w/o TSP: Removing the TSP module.

dataset having one specific component removed. We could see that removing any design of our full model leads to worse performance, proving that our designs could boost the proposed model learning and improve the quality of the generated extrapolation images. We further study the effectiveness of our designs from qualitative results, with some examples shown in Fig. 7. Removing the TSP module could decline the model’s performance, in which the image quality

of the predicted ambient region is unsatisfactory. On the contrary, our full model with introducing the TSP module generates more delicate results with rich texture and exquisite details. The potentially temporal and spatial information could help the model predict more reasonable and coherent content. For example, in the third row of Fig. 7, our full model generates the whole waves smoothly and seamlessly with more consistent details in column (f) compared to other variants having broken waves marked in the orange box. Besides, the beach looks more realistic as well.

Overall, replacing transformer structure with CCN backbone in the variant of CNN with SC&TSP suffers from blur and has an obvious boundary between the input and predicted region due to long-range dependencies not being well extracted. When only using Swin Transformer blocks, the extended image borders have plausible structure but obvious blunt colours in column (c). When further utilizing the SC, more realistic and smooth colours are generated in the extended areas but not satisfactory details in column (d). While not adding SC but a TSP as the bottleneck, there is blurriness but generates vivid details in column (e). In general, only when employing both

SC and TSP in the framework, could the full model be able to extrapolate around images with plausible structure and vivid details as shown in highlighted regions.

5 Conclusion and Future Work

In this paper, we have proposed the transformer-based generative adversarial network (U-Transformer) to improve the generalised image outpainting performance. The Swin Transformer blocks overcame the intrinsic locality and better captured image long-range dependencies. Moreover, the Skip Connection and multi-view Temporal Spatial Predictor modules reinforced image self-reconstruction as well as unknown-part prediction smoothly and realistically. Extensive experiments on scenery and building datasets proved the effectiveness of our methods.

Trained with a fixed resolution, our work may not extrapolate a high-quality image of arbitrary resolution given an input image in the testing stage. In the future, we will investigate to improve the Swin Transformer block making it tractable to handle feature maps with a larger masked part in the testing stage.

References

- [1] Hu Cao, Yueyue Wang, Joy Chen, Dongsheng Jiang, Xiaopeng Zhang, Qi Tian, and Manning Wang. Swin-unet: Unet-like pure transformer for medical image segmentation. *arXiv preprint arXiv:2105.05537*, 2021. [4](#)
- [2] Jieneng Chen, Yongyi Lu, Qihang Yu, Xiangde Luo, Ehsan Adeli, Yan Wang, Le Lu, Alan L Yuille, and Yuyin Zhou. Transunet: Transformers make strong encoders for medical image segmentation. *arXiv preprint arXiv:2102.04306*, 2021. [2](#), [4](#)
- [3] Alexey Dosovitskiy, Lucas Beyer, Alexander Kolesnikov, Dirk Weissenborn, Xiaohua Zhai, Thomas Unterthiner, Mostafa Dehghani, Matthias Minderer, Georg Heigold, Sylvain Gelly, Jakob Uszkoreit, and Neil Houlsby. An image is worth 16x16 words: Transformers for image recognition at scale. In *9th International Conference on Learning Representations, ICLR 2021, Virtual Event, Austria, May 3-7, 2021*, 2021. [2](#), [4](#)
- [4] Benjamin Graham, Alaeldin El-Nouby, Hugo Touvron, Pierre Stock, Armand Joulin, Hervé Jégou, and Matthijs Douze. Levit: a vision transformer in convnet’s clothing for faster inference. *CoRR*, abs/2104.01136, 2021. [4](#)
- [5] Kaiming He, Xiangyu Zhang, Shaoqing Ren, and Jian Sun. Deep residual learning for image recognition. In *Proceedings of the IEEE conference on computer vision and pattern recognition*, pages 770–778, 2016. [8](#)
- [6] Byeongho Heo, Sangdoo Yun, Dongyoon Han, Sanghyuk Chun, Junsuk Choe, and Seong Joon Oh. Rethinking spatial dimensions of vision transformers. *CoRR*, abs/2103.16302, 2021. [4](#)
- [7] Martin Heusel, Hubert Ramsauer, Thomas Unterthiner, Bernhard Nessler, and Sepp Hochreiter. Gans trained by a two time-scale update rule converge to a local nash equilibrium. *Advances in neural information processing systems*, 30, 2017. [7](#)
- [8] Sepp Hochreiter and Jürgen Schmidhuber. Long short-term memory. *Neural computation*, 9(8):1735–1780, 1997. [2](#)
- [9] Han Hu, Jiayuan Gu, Zheng Zhang, Jifeng Dai, and Yichen Wei. Relation networks for object detection. In *Proceedings of the IEEE conference on computer vision and pattern recognition*, pages 3588–3597, 2018. [6](#)
- [10] Han Hu, Zheng Zhang, Zhenda Xie, and Stephen Lin. Local relation networks for image recognition. In *Proceedings of the IEEE/CVF International Conference on Computer Vision*, pages 3464–3473, 2019. [3](#), [6](#)
- [11] Alexia Jolicoeur-Martineau. The relativistic discriminator: a key element missing from standard GAN. In *7th International Conference on Learning Representations, ICLR 2019, New Orleans, LA, USA, May 6-9, 2019*. OpenReview.net, 2019. [3](#), [7](#)
- [12] Kyunghun Kim, Yeohun Yun, Keon-Woo Kang, Kyeongbo Kong, Siyeong Lee, and Suk-Ju Kang. Painting outside as inside: Edge guided image outpainting via bidirectional rearrangement with progressive step learning. In *Proceedings of the IEEE/CVF Winter Conference on Applications of Computer Vision*, pages 2122–2130, 2021. [1](#), [2](#), [3](#)
- [13] Han Lin, Maurice Pagnucco, and Yang Song. Edge guided progressively generative image outpainting.

In *Proceedings of the IEEE/CVF Conference on Computer Vision and Pattern Recognition*, pages 806–815, 2021. 1

[14] Ze Liu, Yutong Lin, Yue Cao, Han Hu, Yixuan Wei, Zheng Zhang, Stephen Lin, and Baining Guo. Swin transformer: Hierarchical vision transformer using shifted windows. *arXiv preprint arXiv:2103.14030*, 2021. 4

[15] Ze Liu, Yutong Lin, Yue Cao, Han Hu, Yixuan Wei, Zheng Zhang, Stephen Lin, and Baining Guo. Swin transformer: Hierarchical vision transformer using shifted windows. *CoRR*, abs/2103.14030, 2021. 5

[16] Chia-Ni Lu, Ya-Chu Chang, and Wei-Chen Chiu. Bridging the visual gap: Wide-range image blending. In *Proceedings of the IEEE/CVF Conference on Computer Vision and Pattern Recognition*, pages 843–851, 2021. 2, 3

[17] Ye Ma, Jin Ma, Min Zhou, Quan Chen, Tiezheng Ge, Yuning Jiang, and Tong Lin. Boosting image outpainting with semantic layout prediction. *arXiv preprint arXiv:2110.09267*, 2021. 3

[18] Roey Mechrez, Itamar Talmi, and Lihi Zelnik-Manor. The contextual loss for image transformation with non-aligned data. In *Proceedings of the European Conference on Computer Vision (ECCV)*, pages 768–783, 2018. 7

[19] Deepak Pathak, Philipp Krahenbuhl, Jeff Donahue, Trevor Darrell, and Alexei A Efros. Context encoders: Feature learning by inpainting. In *Proceedings of the IEEE conference on computer vision and pattern recognition*, pages 2536–2544, 2016. 1

[20] Colin Raffel, Noam Shazeer, Adam Roberts, Katherine Lee, Sharan Narang, Michael Matena, Yanqi Zhou, Wei Li, and Peter J. Liu. Exploring the limits of transfer learning with a unified text-to-text transformer. *J. Mach. Learn. Res.*, 21:140:1–140:67, 2020. 6

[21] Prajit Ramachandran, Niki Parmar, Ashish Vaswani, Irwan Bello, Anselm Levskaya, and Jonathon Shlens. Stand-alone self-attention in vision models. *arXiv preprint arXiv:1906.05909*, 2019. 3

[22] Olaf Ronneberger, Philipp Fischer, and Thomas Brox. U-net: Convolutional networks for biomedical image segmentation. arxiv 2015. *arXiv preprint arXiv:1505.04597*, 2019. 5

[23] Mark Sabini and Gili Rusak. Painting outside the box: Image outpainting with gans. *arXiv preprint arXiv:1808.08483*, 2018. 3

[24] Tim Salimans, Ian Goodfellow, Wojciech Zaremba, Vicki Cheung, Alec Radford, and Xi Chen. Improved techniques for training gans. *Advances in neural information processing systems*, 29:2234–2242, 2016. 7

[25] Karen Simonyan and Andrew Zisserman. Very deep convolutional networks for large-scale image recognition. *arXiv preprint arXiv:1409.1556*, 2014. 7

[26] Basile Van Hoorick. Image outpainting and harmonization using generative adversarial networks. *arXiv preprint arXiv:1912.10960*, 2019. 2, 3, 8

[27] Ashish Vaswani, Noam Shazeer, Niki Parmar, Jakob Uszkoreit, Llion Jones, Aidan N Gomez, Łukasz Kaiser, and Illia Polosukhin. Attention is all you need. In *Advances in neural information processing systems*, pages 5998–6008, 2017. 3

[28] Yi Wang, Xin Tao, Xiaojuan Qi, Xiaoyong Shen, and Jiaya Jia. Image inpainting via generative multi-column convolutional neural networks. In Samy Bengio, Hanna M. Wallach, Hugo Larochelle, Kristen Grauman, Nicolò Cesa-Bianchi, and Roman Garnett, editors, *Advances in Neural Information Processing Systems 31: Annual Conference on Neural Information Processing Systems 2018, NeurIPS 2018, December 3-8, 2018, Montréal, Canada*, pages 329–338, 2018. 7

[29] Yi Wang, Xin Tao, Xiaoyong Shen, and Jiaya Jia. Wide-context semantic image extrapolation. In *Proceedings of the IEEE/CVF Conference on Computer Vision and Pattern Recognition*, pages 1399–1408, 2019. 2, 3, 7, 8

[30] Chao Yang, Xin Lu, Zhe Lin, Eli Shechtman, Oliver Wang, and Hao Li. High-resolution image inpainting using multi-scale neural patch synthesis. In *Proceedings of the IEEE conference on computer vision and pattern recognition*, pages 6721–6729, 2017. 1

[31] Zongxin Yang, Jian Dong, Ping Liu, Yi Yang, and Shuicheng Yan. Very long natural scenery image prediction by outpainting. In *Proceedings of the IEEE/CVF International Conference on Computer Vision*, pages 10561–10570, 2019. 2, 3, 7, 8

[32] Jiahui Yu, Zhe Lin, Jimei Yang, Xiaohui Shen, Xin Lu, and Thomas S Huang. Generative image inpainting with contextual attention. In *Proceedings of the IEEE conference on computer vision and pattern recognition*, pages 5505–5514, 2018. 1

[33] Daquan Zhou, Bingyi Kang, Xiaojie Jin, Linjie Yang, Xiaochen Lian, Qibin Hou, and Jiashi Feng. Deepvit: Towards deeper vision transformer. *CoRR*, abs/2103.11886, 2021. 4